Neurobiology of Disease 140 (2020) 104849

Contents lists available at ScienceDirect

Neurobiology of Disease

journal homepage: www.elsevier.com/locate/ynbdi

Increased transcription of transglutaminase 1 mediates neuronal death in *in vitro* models of neuronal stress and Aβ1–42-mediated toxicity

Debasmita Tripathy[a,1], Alice Migazzi[a,1], Federica Costa[a], Alessandro Roncador[a], Pamela Gatto[a], Federica Fusco[b], Lucia Boeri[c], Diego Albani[b], J. Leon Juárez-Hernández[d], Carlo Musio[d], Laura Colombo[e], Mario Salmona[e], M.M. Micha Wilhelmus[f], Benjamin Drukarch[f], Maria Pennuto[g,h,i], Manuela Basso[a,*]

[a] Department of Cellular, Computational and Integrative Biology - CIBIO, University of Trento, Trento, TN, Italy
[b] Department of Neuroscience, Laboratory of Genetics of Neurodegenerative Disorders, Istituto di Ricerche Farmacologiche Mario Negri IRCCS, Milano, Italy
[c] Department of Chemistry, Materials and Chemical Engineering "G. Natta", Politecnico di Milano, Milan, Italy
[d] Institute of Biophysics, Trento Unit, National Research Council (IBF-CNR), Bruno Kessler Foundation (FBK), LabSSAH, Via alla Cascata 56/C, 38123 Trento, Italy
[e] Department of Molecular Biochemistry and Pharmacology, Laboratory of Pharmacodynamics and Pharmacokinetics, Istituto di Ricerche Farmacologiche Mario Negri IRCCS, Milano, Italy
[f] VU University Medical Center, Neuroscience Campus Amsterdam, Department of Anatomy and Neurosciences, Amsterdam, the Netherlands
[g] Dulbecco Telethon Institute Lab of Neurodegenerative Diseases, Centre for Integrative Biology (CIBIO), University of Trento, Italy
[h] Department of Biomedical sciences, via Ugo Bassi 58/B, University of Padova, 35131 Padova, Italy
[i] Padova Neuroscience Center, 35100 Padova, Italy

ARTICLE INFO

Keywords:
Transglutaminase 1
Alzheimer's disease
Aβ 1–42 peptides
Neuronal death
Activator protein 1

ABSTRACT

Alzheimer's disease (AD) is the most common cause of dementia. At the pre-symptomatic phase of the disease, the processing of the amyloid precursor protein (APP) produces toxic peptides, called amyloid-β 1–42 (Aβ 1–42). The downstream effects of Aβ 1–42 production are not completely uncovered. Here, we report the involvement of transglutaminase 1 (TG1) in *in vitro* AD models of neuronal toxicity. TG1 was increased at late stages of the disease in the hippocampus of a mouse model of AD and in primary cortical neurons undergoing stress. Silencing of *TGM1* gene was sufficient to prevent Aβ-mediated neuronal death. Conversely, its overexpression enhanced cell death. *TGM1* upregulation was mediated at the transcriptional level by an activator protein 1 (AP1) binding site that when mutated halted *TGM1* promoter activation. These results indicate that TG1 acts downstream of Aβ-toxicity, and that its stress-dependent increase makes it suitable for pharmacological intervention.

1. Introduction

Alzheimer's disease (AD) is the most common neurodegenerative disease in individuals older than 60 years of age. The pathological hallmarks of AD are the presence of extracellular plaques, which are mainly composed of abnormally folded amyloid-beta (Aβ) peptides, and intracellular tangles, which are mainly composed of hyper-phosphorylated tau. The strongest evidence for Aβ and tau involvement in AD pathogenesis comes from familial cases of AD where mutations in the amyloid precursor protein (APP) and in genes coding for enzymes involved in its processing, namely presenilin 1 (PSEN1) and PSEN2, were identified. Similarly, mutations in the gene coding for tau have been linked to another neurodegenerative disease, namely frontotemporal dementia, suggesting that alterations in both Aβ and tau homeostasis contribute to neuronal damage and death (Wang and Zhang, 2018). Furthermore, mutant Aβ and tau protein assume a misfolded conformation that influences the structure of normal proteins and mediates spreading of the disease across the brain with a prion-like propagation (Olsson et al., 2018). The mechanisms that lead to protein misfolding and aggregation are still subject of investigation.

TGs are eight calcium-dependent enzymes encoded by closely related genes, namely *TGM1–7*, *F13A1*, and *EPB42* (Basso and Ratan, 2013) that encodes a structural protein that lacks the catalytic core. They are composed of four structurally distinct domains, namely an N-

* Corresponding author at: Laboratory of Transcriptional Neurobiology, Department of Cellular, Computational and Integrative Biology – CIBIO, University of Trento, via Sommarive 9, 38123 Trento, TN, Italy.
E-mail address: manuela.basso@unitn.it (M. Basso).
[1] These authors equally contributed to the work.

https://doi.org/10.1016/j.nbd.2020.104849
Received 20 December 2019; Received in revised form 1 March 2020; Accepted 24 March 2020
Available online 25 March 2020

terminal β-sandwich domain, a catalytic core, and two β-barrel domains. The catalytic core comprises three critical amino acids (cysteine, histidine and aspartic acid), through which TGs binds to glutamine residues to form a stable isopeptide bond between the two substrates, also known as transglutaminase-catalyzed protein crosslinking (Basso and Ratan, 2013; Thomas et al., 2013). Aberrant TG enzymatic activity has been reported in AD and in other neurodegenerative diseases, such as Parkinson's disease (PD) and Huntington's disease (HD)(Grosso et al., 2014; Munsie et al., 2011). The isoenzymes expressed in the brain are TG1, TG2, TG3 and TG6 (Basso and Ratan, 2013); in AD, TG1 and TG2 were observed in intraneuronal deposits in the brain along with a significant (30 to 50-fold) increase in gamma-glutamyl lysine crosslinks relative to control brain (Kim et al., 1999; Wilhelmus et al., 2009), inferring that they contribute to the formation of amyloid deposits (Zhang et al., 1998), and to the crosslinking of tau (Halverson et al., 2005), thereby accelerating the formation of neurofibrillary tangles (Selkoe et al., 1982). Moreover, in PD, TG2 overexpression enhanced the formation of amyloid species of alpha-synuclein *in vivo*, which exacerbated inflammation and neuronal damage (Grosso et al., 2014). Accordingly, TG2 knockout drastically reduced the formation of high molecular weight species of mutant huntingtin in HD (Franich et al., 2018). TG1 and TG2 were shown to be significantly induced also in brain ischemia, and their inhibition or genetic suppression rescued oxidative stress-induced cell loss in immature cortical neurons undergoing ferroptosis (Basso et al., 2012). While TG2 is a ubiquitous protein, TG1 is mostly expressed in the skin where its expression and function have been investigated in the formation of the stratum corneum (Burguera and Love, 2006). The conversion of the upper granule layer cells into the cornified layer involves the activation of TG1, which then participates in the formation of the epidermal barrier (Kalinin et al., 2001), composed of ε-(γ-glutamyl) lysine cross-linked proteins, hallmarks of TG-catalyzed reactions (Basso and Ratan, 2013; Thomas et al., 2013). Lately its expression has been reported in brain, lung, heart, kidney and liver (Martinet et al., 2003; Li et al., 2016; Baumgartner et al., 2004; Zhang et al., 2009; Ponnusamy et al., 2009). For the first time, here we show that TG1 is transcriptionally upregulated in the hippocampus of AD mice at late stages of the disease. TG1 upregulation is observed in cortical neurons *in vitro* upon glutamate or Aβ 1–42 peptide treatment. TG1 is necessary and sufficient to cause toxicity in *in vitro* model of AD, and its transcriptional increase is mediated by the binding of the activator protein 1 (AP1)-responsive elements at the *TGM1* promoter. These results suggest TG1 as a possible target for AD pathogenesis and confirm AP1 and the mitogen-activated protein kinase (MAPK) pathway as important mediators of AD pathogenesis.

2. Materials and methods

2.1. Animals

Homozygous 3xTg-AD mice (and non-transgenic strain-matched control line, ctrl) were kindly provided by Dr. S. Oddo to the laboratory of Dr. Albani (Oddo et al., 2003). Mice were housed at 23 °C room temperature with food and water *ad libitum* and a 12-h light/dark cycle. Animal care and experimental procedures were conducted in accordance with the Istituto di Ricerche Farmacologiche Mario Negri IRCSS (IRFMN, authorization number 28/2016-PR) and the University of Trento ethics committee. Primary mouse cortical neurons were obtained from C57BL/6 J wild type embryos at day 15 (E15.5).

2.2. Immunohistochemistry

Animals were euthanized at the desired age through cervical dislocation. The brain was harvested and dissected on ice. After dissection, the brains were immediately stored at −80 °C until use. Serial coronal sections of 10 μm were obtained, starting at the base of the hippocampus. The acquired sections were fixed for 20 min using 4% paraformaldehyde (0.1 M phosphate buffer, pH 7.4). Endogenous peroxidases were quenched using a 0.3% H_2O_2, 0.1% sodium azide solution in tris-buffered saline (TBS, pH 7.6), this was done for 15 min. Nonspecific sites were blocked using 3% normal donkey serum (Jackson Immunoresearch Laboratories Inc., Suffolk, UK). All sections were incubated with their primary antibodies for 48 h at 4 °C. All primary antibodies were diluted in a TBS-Triton (0.5% Triton X-100) solution. Between the different incubation steps, sections were washed with TBS. The sections were stained for amyloid-beta using a rabbit anti-human anti-amyloid antibody (#715800, dilution 1/100) purchased from Invitrogen (Carlsbad, CA, USA). To stain hyper-phosphorylated tau, a mouse anti-human antibody recognizing tau protein phosphorylated at both serine 202 and threonine 205 sites (AT8, dilution 1/3000), obtained from Innogenetics (Zwijnaarde, Belgium) was used. Goat anti-human TG1 antibody (directed against the N-terminal parts of the protein, dilution 1/100) was purchased from Santa Cruz Biotechnology (Santa Cruz, CA, USA). Negative controls for immunostainings were generated by omission of primary antibodies. Primary antibody signal was enhanced using Immpress® mouse alkaline phosphatase and Immpress® goat-horseradish peroxidase (Vector Laboratories, Burlingame, CA), followed by chromogens liquid permanent with 10 min incubation with Vector®SG (Vector Laboratories). Finally, slides were rinsed by 3x5min TBS-HCl and mounted using Mowiol (Sigma-Aldrich, Zwijndrecht, The Netherlands). Analysis was performed using a Leica CTR5000 light microscope (Leica Microsystems, Rijswijk, the Netherlands) combined with the spectral imager Nuance 3.0.2. purchased from PerkinElmer (Waltham, MA, USA).

2.3. Cortical neuron culture

Cortices from embryonic E15.5 C57BL/6 J mice were dissected out, digested in papain solution (20 U papain, 5-mM EDTA and 30 mM cystine in 1× Earle's Balanced Salt Solution (EBSS)) for 20 min. This was followed by a DNase I treatment for 3 min. The dissociated cells were centrifuged at 1000 ×*g* for 5 min. Supernatant was discarded and the digestion was blocked with a solution containing trypsin inhibitor and bovine serum albumin in EBSS. Following a centrifugation of 1000 ×*g* for 10 min the cells were plated in MEM media supplemented with 10% fetal bovine serum, L-glutamine (2 mM) and pen-strep (1%). The day after half the media was replaced with Neurobasal medium supplemented with B27, pen-strep (1%), L-glutamine (2 mM), sodium pyruvate (1 mM) and AraC (8 μM). Half of the media was replaced with fresh media every 3 days (Basso et al., 2012).

2.4. Excitotoxicity model for cell death

L-glutamic acid (Sigma-Aldrich #G5889) was dissolved in phosphate buffered saline at a stock concentration of 250 mM, serial dilutions were done in the Neurobasal medium. Mature primary cortical neurons, at DIV7, were treated with three different concentrations of glutamate: 1 μM, 5 μM and 30 μM. Glutamate was added to the medium for 5 min and then the entire medium was changed with fresh supplemented Neurobasal medium as described above. 24 h after treatment, the neurons were harvested for further analysis.

2.5. Amyloid β 1–42 –induced neurotoxicity

Lyophilized Aβ 1–42 peptides were re-suspended with NaOH 10 mM and diluted in Neurobasal medium to obtain Aβ 1–42 monomers (Manzoni et al., 2009). For the neuronal viability experiments they were diluted at concentrations of 0.25 μM, 0.5 μM and 1 μM. For other experiments they were used at 0.5 μM. Once ready they were added to the neurons and left for 72 h.

2.6. TG1 over-expression

TG1 was cloned into the LentiLox 3.7 backbone under the control of the synapsin I promoter to generate the *syn*-eGFP_TGM1 plasmid, used for overexpression studies. This construct contained two ORFs with two independent synapsin promoters: synPr I (driving TGM1 gene) and synPr II (driving eGFP gene); synapsin promoters are highly specific for neuronal expression. The syn-eGFP construct was used as negative control. These plasmids were then expressed in HEK293T cells together with pCMV-dR8.91 (Delta 8.9) plasmid containing *gag*, *pol* and *rev* genes and VSV-G envelope plasmid for production of viral particles. On day2 the medium was changed to fresh DMEM with supplements. The supernatant was collected on day3 the medium was collected, spun down to discard cellular debris filtered (0.45 μm pore size filters) and stored at −80 °C in aliquots, until use. Before infection the virus titer was quantified using the SG-PERT reverse transcription assay (Pizzato et al., 2015) as described in (Tripathy et al., 2017). Viruses were added to the neurons at DIV0 at multiplicity of infection (MOI) 3 and the effect of overexpression was evaluated at DIV8. To calculate the transduction efficiency, we counted the percentage of GFP-positive neurons over total neurons. 66.2 ± 3.5% and 62.2 ± 8.9% of neurons were transduced in the synGFP and synGFP-TG1 samples, respectively.

2.7. TG1 silencing

Four different shTG1 constructs and a non-target shRNA control vector – sh scrambled (Sigma) were tested on HT22 using the Lipofectamine® LTX DNA transfection reagents. The cells were analyzed 48 h after the transfection (data not shown) and the most efficient shTG1, *i.e.*, shRNA2 (GCGGCAAGAATATGTGCTTAA), was used on neurons for TG1 knockdown experiments. The scrambled shRNA was used as a negative control. Neurons were treated with lentiviruses expressing a scrambled shRNA or shRNA-TG1 at DIV0 at MOI 3 and analyzed at DIV8. The preparation and titration of viruses was done as mentioned above.

2.8. Immunofluorescence (IF)

For IF, neurons were grown on coverslips coated with poly-D-lysine (0.01 mg/ml in PBS). At DIV8, the coverslips were fixed using 4% paraformaldehyde prepared in phosphate buffered saline (PBS). This was followed by three washes in PBS (5 min each) and then incubation with 0.1% Triton X-100 (in PBS) for 5 min, to allow permeabilization. After the permeabilization, coverslips were washed in PBS (5 min each) three times. The blocking solution (10% FBS, 0,05% of Triton X-100 in PBS) was then added for 1 h. Neurons were then incubated overnight with the primary antibody (TG1 (1:100), MAP2 (1:500), GFP (1:1000)) diluted in 0.01% of FBS in PBS. The next day, after three washes in PBS, the secondary antibody (anti-rabbit Alexa Fluor® 568 and anti-mouse Alexa Fluor® 488 1:1000) in 0.01% of FBS in PBS was added for 1 h, in dark. Following 3 washes in PBS (5 min each), coverslips were mounted on glass slides with ProLong Gold antifade mounting media containing the nuclear stain, DAPI (Life Technologies). Slides were imaged with Zeiss AxioObserver Z1 microscope.

2.9. Neuronal viability assays

Primary cortical neurons were plated in 96-well plates at a density of $0.25*10^6$/ml (plating volume 100 μl per well). When needed, the immature neurons were transduced at DIV0 at MOI 3. Following desired treatments, the neurons were fixed and processed for immunocytochemistry as described above. Following washes after the secondary antibody, cells were incubated with Hoechst dye (1:1500 in PBS) for 10 min. This was followed by one wash with PBS and addition of fresh PBS for image acquisition. The plates were imaged with Operetta™ high-content screening system (PerkinElmer). In each well, images were acquired in preselected fields (12) with LWD 20× objective over three channels with the following filter settings: λ = 360–400 nm excitation/λ = 410–480 nm emission for Hoechst, λ = 460–490 nm excitation/λ = 500–550 nm emission for anti-GFP antibody revealed by Alexa Fluor® 488 and λ = 520–550 nm excitation/λ = 590–640 nm emission for anti-MAP2 antibody revealed by Alexa Fluor® 568. The images were analyzed using the Harmony software version 4.1 (PerkinElmer). Based on Hoechst staining and Alexa Fluor® 568 fluorescence intensity, nuclei and cytoplasm were respectively identified. In each assay, the total number of GFP^+ or $MAP2^+$ alive neurons in each condition was counted. The experiments were carried out in triplicates and repeated at least three times independently.

2.10. Immunoblotting

Neurons were plated in 6-well plates at a density of $0.5*10^6$/ml (plating volume 2 ml per well). At DIV8, neurons were lysed using 1% Triton lysis buffer (25 mM Tris-HCl pH 7.4, 100 mM NaCl, 1 mM EGTA, 1% Triton X-100, protease and phosphatase inhibitors). The lysis volume was maintained at 45 μl and the total volume was used for SDS-PAGE. Primary antibodies (anti-TG1, Cloud-clone Corp #PAB773Mu02 1:500; anti-GFP, Life Technologies #A10262 1:1000, anti-tubulin, Sigma #T7816 1:10000) were incubated in 5% milk in TBS-Tween 0,1% overnight at 4 °C. InfraRed dye-conjugated or HRP-conjugated secondary antibodies (1:10000 in the blocking solution) were incubated for 1 h at RT and proteins were detected by an Odyssey infrared imaging system (LI-COR Biosciences) or ChemidocTM (Bio-Rad), respectively.

2.11. Quantitative PCR

Total RNA was obtained from cells following the manufacturer instructions using TRIzol (Invitrogen). 1 μg of RNA was reverse transcribed using iScript reverse transcription Supermix (Bio-Rad). The cDNA was diluted 10 times and then 1 μl was used for qPCR using the iTaq universal SYBR green supermix (Bio-Rad). The primer efficiency was calculated for each set of primers and the primers with efficiency approximately 1 were used for the study. Primer used: TG1 Fwd: TGT GGAGATCCTGCTCAGCTACCTA, TG1 Rev.: TGTCTGTGTCGTGTGCAG AGTTGA, GAPDH Fwd: AACCTGCCAAGTATGATGA, GAPDH Rev.: GGAGTTGCTGTTGAAGTC.

2.12. TG1 promoter activity

Different lengths of the TG1 promoter (−0.8 kb, −1.25 kb, −2.2 kb) were cloned into the pGL3 luciferase reporter vector using the restriction sites *Nhe*I and *Bgl*II. Neurons at DIV8 were transfected with TG1 promoter plasmids using Lipofectamine2000 (Life Technologies). The following day neurons were treated with 0.5 μM Aβ peptides. 24 h post treatment the cells were lysed for transcriptional assay. The assay was performed using the kit Dual-Luciferase (R) Reporter Assay System (Promega) following the manufacturers protocol. The promoter was screened for transcription factor binding sites using the ECR browser and AP1 binding site (TAAGTCA) present at the −1.25 kb promoter was mutated (to TAAAAAA) by site directed mutagenesis.

2.13. Electrophysiology

The following protocols have been adapted from standards already effectively applied to primary cortical neurons (Roncador et al., 2017), motor neuron-derived MN-1 cells (Jimenez Garduno et al., 2017) and SH-SY5Y human neuroblastoma cell (Caponi et al., 2016). Patch-clamp recordings in whole-cell configuration were performed at non-sterile conditions and at room temperature (~20 °C) on mouse cortical neurons, cultured as above described. Once Petri dishes containing cells

were placed and inspected under the set-up's microscope Nikon FN1 (Nikon Instruments, Italy branch, Firenze, Italy), the culture medium was exchanged with the extracellular solution. In order to evoke total currents, pipettes were filled with high potassium solution and a standard Tyrode's formulation was used for extracellular (bath) solution (see below). Patch micropipettes were pulled from GB150-8p (OD 1.5 mm, ID 0.86 mm) borosilicate glass capillaries (Science Product, Hofheim, Germany) using a PIP6 temperature-controlled pipette puller (HEKA, Lambrecht/Pfalz, Germany). Pipettes' resistance ranged from 3 to 7 MΩ. Once the gigaseal was obtained (electric resistance > 1 GΩ), whole-cell configuration was accomplished through the rupture of the patch seal. Holding potential was set to −40 mV, 15 steps of +10 mV (100 ms duration, 1 Hz frequency) were applied starting at −100 mV and voltage drift was eliminated computationally. Bioelectric signals were picked up using a universal voltage/current clamp amplifier (ELC-03XS, npi, Tamm, Germany) connected to a PC computer *via* a breakout-box interface (INT-20, npi, Tamm, Germany). Pipettes were mounted in a piezo-drive micromanipulator (Sensapex, Oulu, Finland). Instant patch clamp parameters (*e.g.*, Rpipette, Rseal, Cm, Gaccess, Gm) were monitored with the signal acquisition software (WinWCP Electrophysiology Software, ©John Dempster, University of Stratchlyde, Scotland), and voltage commands and current responses values were stored in a PC. Signals and monitored parameters were processed off-line and values of IV curves were obtained with semi-automatic algorithm protocols written in MATLAB (Mathworks, USA). The values of the steady-state current (around 50–70 data points averaged and located at the final part of the current response recorded during the voltage stimulus) were calculated at a given command potential and used to compare the different samples. This relationship was completed with series of averaged current responses obtained from successful recordings. Extracellular (bath) solution contained: NaCl, 136.4 mM; KCl, 5.4 mM; $CaCl_2$, 1.8 mM; $MgCl_2$, 0.53 mM; HEPES 5.5 mM and glucose 5.5 mM; pH 7.4 with NaOH. Internal (pipette) solution contained: K acetate, 130 mM; KCl, 20 mM; KH_2PO_4, 1 mM; $MgCl_2$, 1 mM; HEPES, 5 mM; EGTA, 0.1 mM; ATP−Na, 1 mM and GTP-Na, 0.1 mM; pH 7.2 with KOH.

3. Results

3.1. Up-regulation of TG1 levels in 3xTg hippocampus

Elevated levels of TG1 in the brain of AD patients were previously reported (Kim et al., 1999) along with a specific accumulation of TG1 in hyperphosphorylated tau inclusions (Wilhelmus et al., 2012). We wondered whether TG1 levels were upregulated in a mouse model of AD. We used the 3xTg-AD mice, which harbor PS1(M146V), APP(Swe), and tau(P301L) transgenes and accumulate over time amyloid plaques and tau tangles, mainly in the hippocampus and cortex, with an evident pathologic profile starting from 12 months. Moreover, beginning from 4 months of age, 3xTg-AD mice show cognitive impairment deriving from early synaptic dysfunction, but with no diffuse brain deposits (Oddo et al., 2003). We analyzed the transcript levels of TG1 mRNA by real-time (RT)-PCR in the hippocampus at different time-points (Calderon-Garciduenas and Duyckaerts, 2017). TG1 mRNA levels showed a 5-fold increase in 3xTg-AD mice compared to strain-matched non-transgenic controls at 18 months (Fig. 1A). No significant difference in TG1 mRNA levels was observed at 4 months and 8 months between control and AD mice.

We further validated the increase of TG1 expression in AD mice by immunohistochemistry analysis in 18-month old control and transgenic AD mice. Anti-TG1 antibody immunoreactivity was observed in a subset of neurons throughout the murine brain and in neurons of the nuclear layer in the cortex (not shown). In transgenic mice, extensive Aβ and hyperphosphorylated tau pathology was observed throughout the brain and in the hippocampus (Fig. 1B, C, E, F, H). TG1 expression was also detected in a subset of neurons in the nuclear layer of the hippocampus

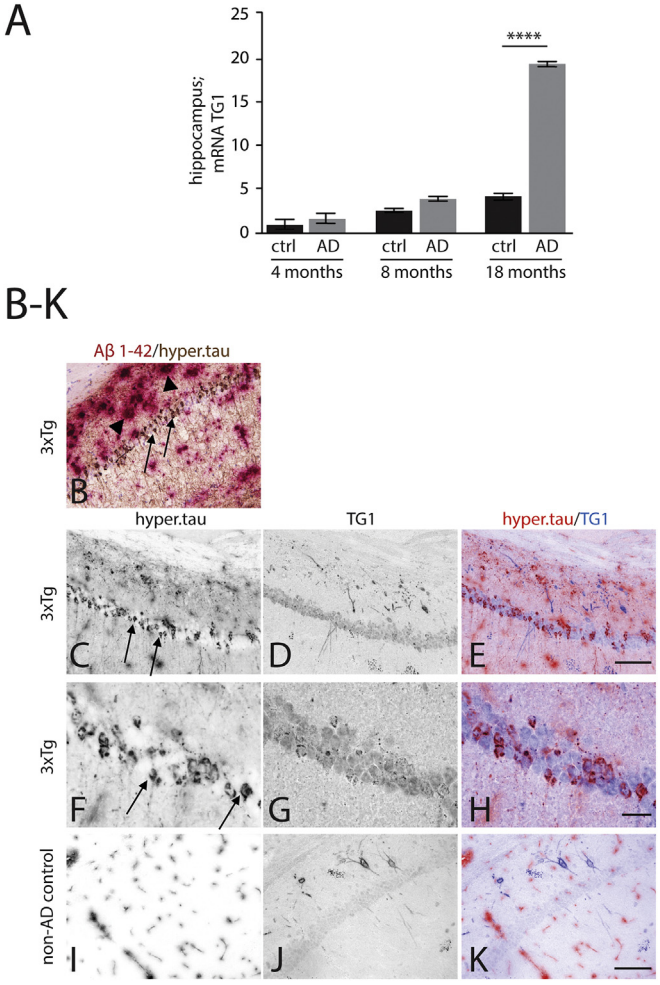

Fig. 1. TG1 expression. (A) Significant up-regulation of TG1 gene expression in the hippocampus of old (18 months) 3xTg AD mice, as compared to age matched control. Graph represented as mean ± SEM, ****P < .0001, one-way ANOVA with Tukey's *post hoc* test. B−K) Colocalization of TG1 with hyperphosphorylated tau inclusions in an AD mouse model (B) Anti-Aβ and anti-hyperphosphorylated tau antibody staining showing Aβ plaques (B, arrowhead) and neuronal hyperphosphorylated tau (B, C and F, arrows) in the 3xTg AD mice, respectively. Anti-TG1 antibody immunoreactivity was observed in neurons of the nuclear layer and in a subset of neurons adjacent to this layer (D). Colocalization of the anti-hyperphosphorylated tau and the anti-TG1 antibody was found in neurons affected by hyperphosphorylated tau within the nuclear layer (E). Magnified pictures in F, G and H corresponding to C, D and E, respectively. (J) No immunoreactivity for anti-Aβ and anti-hyperphosphorylated tau antibody staining was revealed in control hippocampus. Magnification: 20× for B, C-E and I−K, 200 μm bar, 63× for F−H, 15 μm bar.

in control mice (Fig. 1J). Of note, double light microscopical staining excluded TG1 in Aβ pathological lesions (not shown). However, double staining with anti-TG1 and anti-hyperphosphorylated tau antibodies showed localization of TG1 in hyperphosphorylated tau inclusions in affected hippocampal neurons (Fig. 1C–E). Higher power magnification confirmed this observation and, in addition, demonstrated increased immunoreactivity of the anti-TG1 antibody in neurons affected by hyperphosphorylated tau inclusions (Fig. 1G-H). In control animals, hyperphosphorylated tau inclusions were not observed, and the TG1 immunoreactivity in neurons of the nuclear layer was absent (Fig. 1I-K).

3.2. Up-regulation of TG1 levels in stress condition

We wondered whether TG1 increase is neuronal-specific in the brain. We treated DIV8 cortical neurons with increasing concentrations

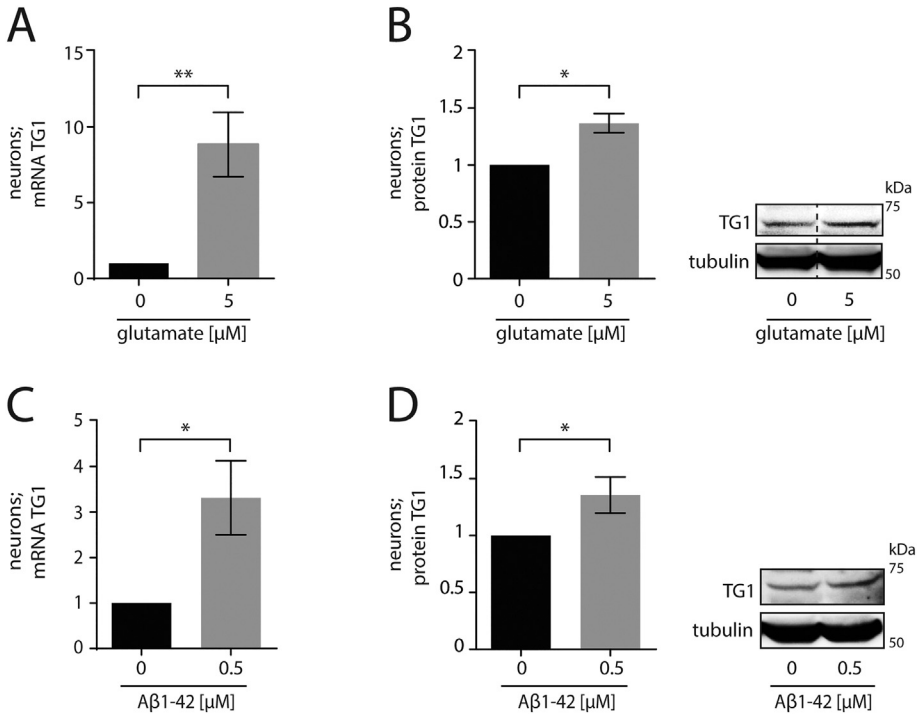

Fig. 2. Stress-induced increase in TG1. (A-B) Excitotoxic stress induced increase in TG1 mRNA (A) and protein (B) levels in primary cortical neurons. Graphs represented as mean ± SEM, n = 3, **P < .01, Student's *t*-test. Dashed line in (B): lanes were run on the same gel, but were noncontiguous. The original blot is shown in Supplementary Fig. 2A. 100 μg of protein lysate were loaded in each lane of the gel. (C-D) Aβ-amyloid treatment significantly increased TG1 mRNA (C) and protein (D) levels in primary cortical neurons. Graph represented as mean ± SEM, n = 3, *P < .05, Student's t-test. The three independent replicates of the immunoblot analysis are shown in Supplementary Fig. 2B. 100 μg of protein lysate were loaded in each lane of the gel.

of glutamate (1 μM, 5 μM, and 30 μM) and Aβ1–42 peptide (0.25 μM, 0.5 μM and 1 μM), two different toxic stimuli involved in AD pathogenesis(Piccini et al., 2012). Upon glutamate treatment, we observed a dose-dependent reduction in neuronal viability of 6%, 52% and 87% respectively (Supplementary Fig. 1A). We found that neurons treated with 5 μM glutamate showed 8-fold increase in TG1 mRNA levels compared to control neurons (Fig. 2A) and a 1.3-fold increase was also observed at the protein level (Fig. 2B, Supplementary Fig. 2A). Similarly, the treatment with Aβ 1–42 reduced neuron viability by 15%, 27% and 37% at doses 0.25 μM, 0.5 μM and 1 μM, respectively (Supplementary Fig. 1B). In neurons treated with 0.5 μM Aβ-amyloid, TG1 mRNA levels showed a statistically significant 3-fold increase (Fig. 2C), while the protein showed a 1.3-fold increase compared to untreated neurons (Fig. 2D, Supplementary Fig. 2B). Collectively, these results show that TG1 is upregulated in AD pathology upon stress, suggesting a direct involvement of TG1 in neuronal toxicity.

3.3. Overexpression of TG1 is sufficient to induce toxicity

TG1 overexpression in immature primary neurons was previously shown to cause cell death (Basso et al., 2012). To determine whether increased TG1 expression exerts toxicity in mature cortical neurons, we generated a lentiviral vector expressing human TG1 and GFP under the control of two independent synapsin promoters. We transduced primary cortical neurons, we confirmed the expression of TG1 by immunofluorescence and immunoblotting experiments (Fig. 3A-B, Supplementary Fig. 3), and we measured cell viability (Fig. 3C). In particular, we performed immunostaining on DIV8 neurons and quantified the number of viable neurons expressing GFP with the Operetta® high content imaging system(Tripathy et al., 2017). We found that overexpression of TG1 reduced neuronal viability by 30% when compared to the control group (Fig. 3C). The neuronal toxicity caused by TG1 overexpression was also confirmed by patch-clamp electrophysiology. Neuronal excitability of mock (synGFP) and TG1-overexpressing neurons was evaluated *in vitro* quantifying the total cell membrane currents by patch clamp in whole-cell modality. Macroscopic currents (*i.e.*, total cell membrane current) were evoked using standard physiological conditions and application of voltage stimulus in order to measure the inwards and outwards currents, mainly ascribed respectively to Na^+, Ca^{++}, and K^+ ion channels. After eight days of *in vitro* maturation, GFP-expressing neurons responded with an average current peak of ~ 0.6 nA at maximum depolarization (step +40 mV), inward and outward components were extended and similar to control neurons (control data not included) (Fig. 3D). On the other hand, the TG1-overexpressing neurons showed a loss of amplitude even at maximum depolarization: ~ 0.2 nA (step +40 mV) and reduced inward and outward components (Fig. 3D). The current-voltage relationship based on the mean of the calculation of the recorded steady-state currents confirmed that TG1-overexpressing neurons had a dramatic reduction of current amplitude, in the outward component, almost approaching to zero value. This condition also resulted in a considerable reduction in the inward component. Beside the components, the rectification behavior (*i.e.*, the change of conductance with voltage) was lost, indicating a substantial alteration of the voltage-dependent gating (Fig. 3E). Altogether, our data show that neurons overexpressing TG1 exhibited a remarkable alteration of the membrane excitability, concerning loss of ionic currents.

3.4. Silencing TG1 protects neurons against stress-induced cell death

To define a causative role for TG1 increased expression in AD hippocampus, we took advantage of an *in vitro* model of AD toxicity by culturing primary neurons in which TG1 was silenced. ShRNA-mediated knockdown of TG1 levels was confirmed by quantitative PCR, which showed a 3.5-fold reduction in TG1 mRNA levels as compared to scrambled shRNA (Fig. 4A) and to a 1.5-fold decrease in TG1 protein levels (Fig. 4B, Supplementary Fig. 4). We treated the neurons with a concentration of glutamate (30 μM) and Aβ-amyloid peptides (0.5 μM) able to induce neuronal death and counted the number of viable neurons with the Operetta® high content imaging system. Notably, while glutamate reduced the viability of scrambled transduced neurons by 60%, the neurons transduced with TG1 shRNA were protected from death (Fig. 4C-D). Similar results were obtained after treatment with Aβ-amyloid peptides. Scrambled-transduced neurons showed a 40% reduction in cell viability while no cell death was observed in neurons transduced with TG1 shRNA (Fig. 4E-F). These observations indicate

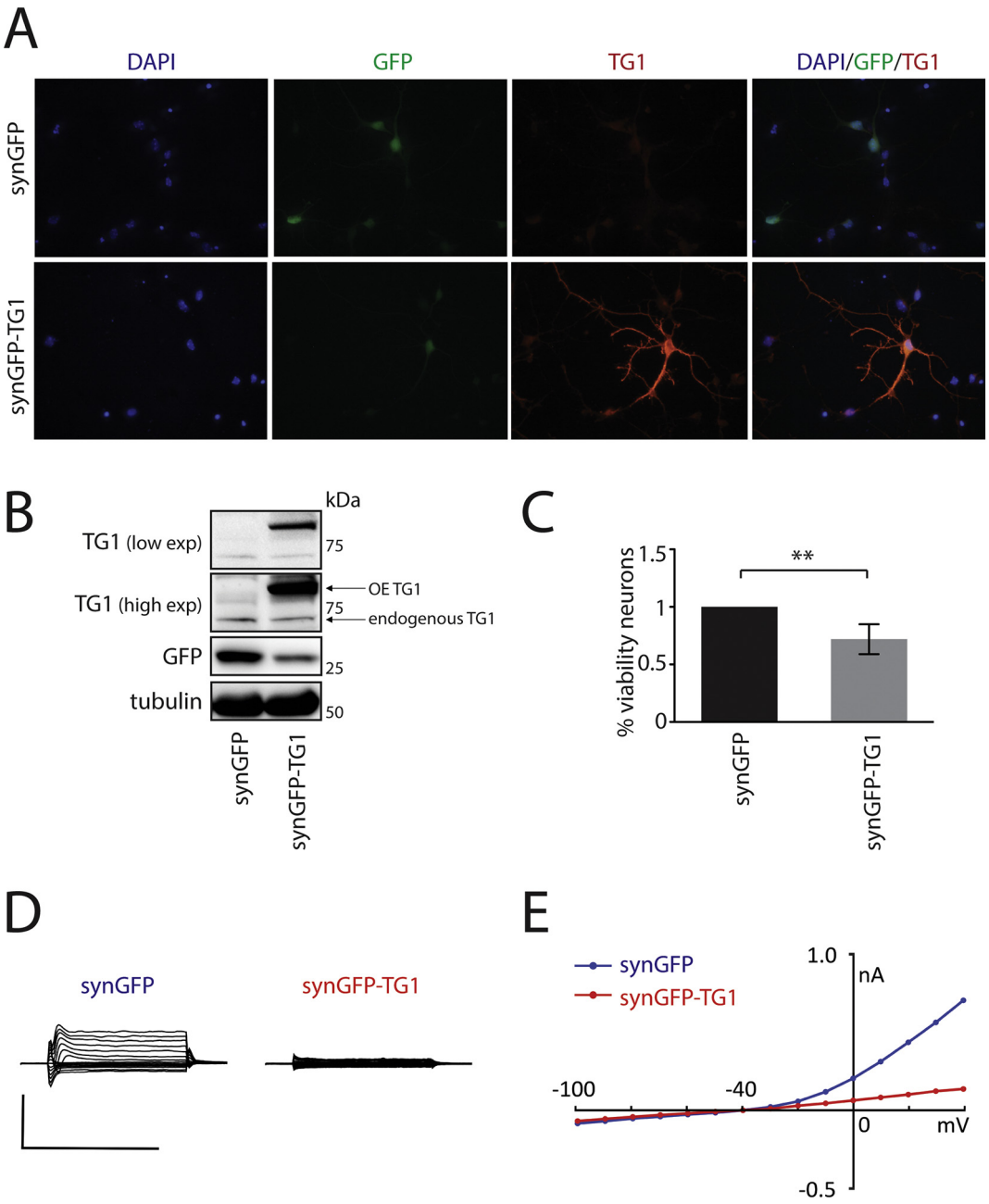

Fig. 3. Overexpression of TG1 induces toxicity. (A) Lentivirus mediated over-expression of TG1 (red). GFP is used as a marker for transduced neurons and DAPI stains the nuclei. (B) Immunoblot showing overexpression of TG1 in neurons transduced with a lentivirus expressing synGFP-TG1 as compared to synGFP alone. The three independent replicates are shown in Supplementary Fig. 3. 100 μg of protein lysate were loaded in each lane of the gel. (C) Reduced viability of neurons infected with synGFP-TG1 virus as compared to those with synGFP alone. Graph represented as mean ± SEM, n = 9, **P < .01, Student's t-test. (D) Examples of whole-cell total currents obtained from control cortical cells (synGFP) at 7 days after plating. Toxicity effect by TG1 in synGFP-TG1 cells is evidently showed by a marked amplitude reduction in the total currents. (E) current-voltage relationship (IV curve) showing the response (current in nA) of the cells to the applied stimulus (voltage in mV) for the four different cell conditions showed in D. For synGFP-TG1 cells the flow of the total currents results dramatically reduced in both inward and outward components. Calibration bar in D: horizontal, 100 ms; vertical, 1 nA. (For interpretation of the references to colour in this figure legend, the reader is referred to the web version of this article.)

that TG1 is necessary for the death of cortical neurons in an *in vitro* model of AD.

3.5. Stress-induced increase in TG1 promoter activity is mediated by AP1

To decipher the mechanism underlining TG1 upregulation, we cloned a series of *TGM1* promoter-luciferase reporter constructs with progressively shorter promoter regions (−2.2 kb, −1.25 kb, −0.8 kb) (Fig. 5A). We transfected the promoter reporters in primary cortical neurons at DIV7 and detected the promoter activity after treatment with Aβ-amyloid peptides (0.5 μM). Interestingly, the −1.25 kb and − 2.2 kb promoter reporters showed increased luciferase activity after treatment with Aβ-amyloid peptides, while the −0.8 kb promoter reporter activity did not change upon treatment (Fig. 5C). These results suggested that the promoter region modulated by Aβ-amyloid peptides spanned between −0.8 kb and − 1.25 kb. Interestingly, we identified an AP1 binding site in the *TGM1* promoter (Fig. 5B) at −0.848 kb (Phillips et al., 2004). AP1 responsive elements are usually bound by c-

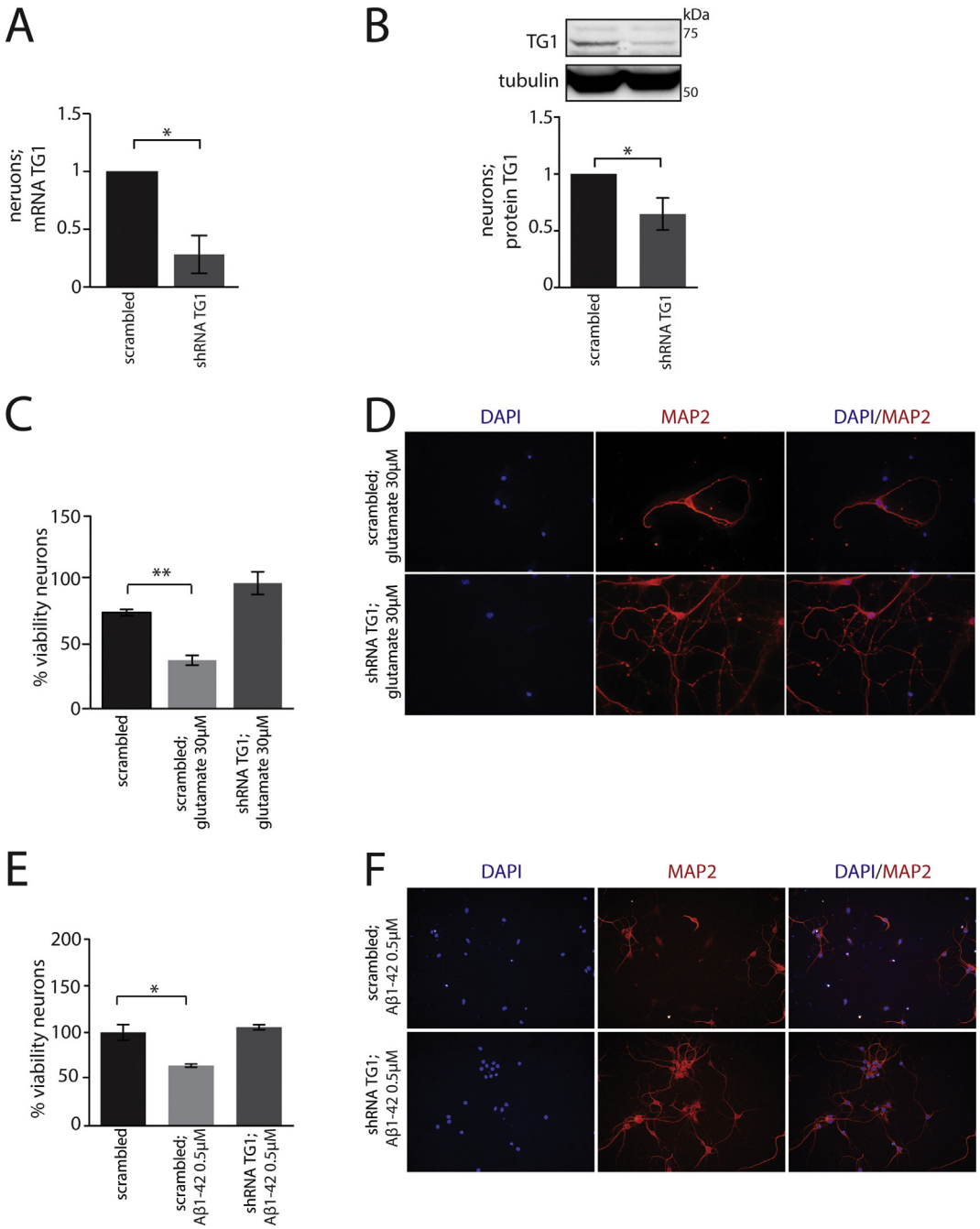

Fig. 4. Knockdown of TG1 provides stress resistance. (A-B) Lentiviruses expressing an shRNA against TG1 were able to reduce the mRNA (A) and protein (B) levels of TG1. Graphs represented as mean ± SEM, n = 3, *P < .05, Student's t-test. The three independent replicates of the immunoblot analysis are shown in Supplementary Fig. 4. 100 μg of protein lysate were loaded in each lane of the gel. (C) Silencing of TG1 rescued primary cortical neurons against glutamate-induced toxicity. Graph represented as mean ± SEM, n = 4, *P < .05, one-way ANOVA with Tukey's *post hoc* test. (D) Representative images for cortical neurons showing increased survival after excitotoxic stress in the TG1 silenced group. (E) Silencing of TG1 rescued primary cortical neurons against Aβ-induced toxicity. Graph represented as mean ± SEM, n = 4, *P < .05, one-way ANOVA with Tukey's *post hoc* test. (F) Representative images showing that TG1 silencing protects against Aβ toxicity.

jun and fos and AP1 acts downstream of the c-jun pathway mediating death signaling in AD (Akhter et al., 2015). We mutagenized the AP1 responsive element (Fig. 5B) and observed that the −1.25 kb promoter reporter activity did not increase upon treatment with Aβ-amyloid peptides (Fig. 5C). These results suggest that *TGM1* upregulation is mediated through AP1 binding by c-jun and fos.

4. Discussion

4.1. TGs and neurodegeneration

In this study, we propose TG1 as a new player in AD pathogenesis and a novel potential pharmacological target for neurodegenerative diseases. TGs have been investigated in several chronic and acute neurodegenerative diseases such as AD, PD, amyotrophic lateral sclerosis, traumatic brain injury and ischemia for the upregulation of

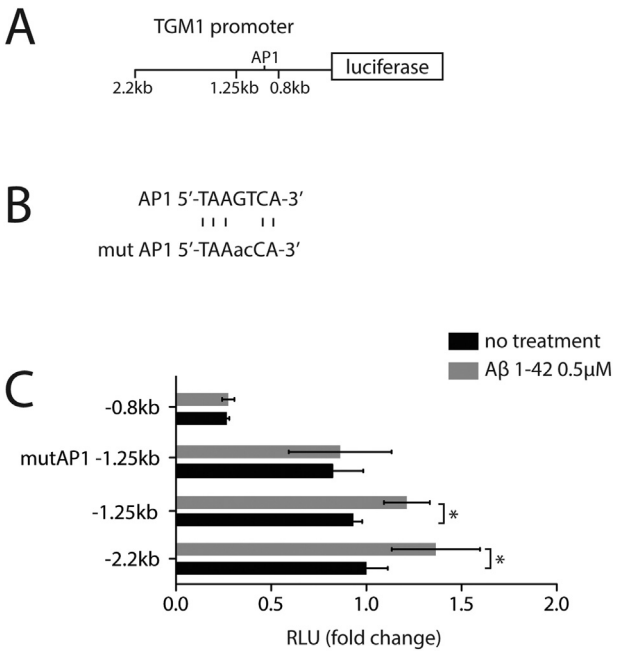

Fig. 5. Induction of TG1 expression is mediated downstream of AP1. (A) Schematic diagram of the different lengths of TG1 promoter cloned with luciferase-reporter constructs. (B) Sequence for the AP1 responsive element at the *TGM1* promoter and the mutation inserted in our construct. (C) TG1 promoter activity upon treatment with Aβ peptides was high for the −2.2 kb and −1.25 kb, and the activity was lost by mutating the AP1 site. Graph represented as mean ± SEM, *P < .05, two-way ANOVA with Bonferroni's *post hoc* test.

their protein levels and the activation of their catalytic activity, which accelerates the formation of oligomers and amyloid structures (Jeitner et al., 2009a; Jeitner et al., 2009b; Bailey et al., 2005). Recently, a proteomic study in brain homogenates identified huntingtin, APP and α-synuclein as the major substrates of TG protein crosslinking (Andre et al., 2017), confirming TG enzymatic activity as an important player in protein aggregation and neurodegeneration. TG1, TG2 and TG3 are three different isoenzymes expressed in the brain that contribute to the elevation of TG transamidase activity. It has been shown that TG2 overexpression induces the formation of high molecular weight aggregates of α-synuclein *in vitro* and *in vivo* in PD (Grosso et al., 2014; Junn et al., 2003) and it increases Aβ oligomerization and neurofibrillary tangle formation in AD (Schmid et al., 2011; Appelt and Balin, 1997). Moreover, TG2 upregulation was reported in post-mortem AD brains and its activation reduced ApoE soluble levels in AD mouse models (Wilhelmus et al., 2009; Zhang et al., 2016; de Jager et al., 2015). TG2 knockout failed to alleviate HD pathology in R6/2 mice, an aggressive model of HD (Menalled et al., 2014), and its overexpression did not accelerate HD pathology *in vivo* (Kumar et al., 2012) but the inhibition of its enzymatic activity halted neurodegeneration (Bailey and Johnson, 2006; Van Raamsdonk et al., 2005). Accordingly, we recently showed that TG2 is sufficient but not necessary for neuronal death in ischemia *in vitro* and *in vivo* (Basso et al., 2012). At the same time, we and others reported that TG transamidase activity is highly activated in ischemic stroke and in oxidative stress-mediated death in immature cortical neurons. This increase in transamidase activity correlates with an increase in TG1 levels. TG1 was also shown to be upregulated in AD human tissues (Wilhelmus et al., 2009; Wilhelmus et al., 2012) and here we demonstrate that in *in vitro* models of neuronal death relevant for AD, TG1 is necessary and sufficient for neuronal toxicity upon excitotoxicity and Aβ treatment. It is plausible to speculate that increased TG1 levels contribute to aberrant protein crosslinking in AD and neuronal death. Similarly, another TG isoenzyme, TG6, is less stable when mutated, it is fast degraded and contributes to Purkinje cells degeneration in spinocerebellar ataxia 35 (Tripathy et al., 2017). TG1 levels are usually very low in the brain, suggesting that TG1 expression is tightly regulated in neuronal cells. Here, upon stress conditions we observed an 8-fold increase of TG1 mRNA levels that only translated into a 1.3-fold induction at the protein level. Further studies on possible mechanisms of TG1 mRNA degradation or post transcriptional regulation by specific microRNAs are warranted. Mir-19, miR-1285, miR-181a and miR-218 were shown to impact TG2 protein levels in various types of cancer (Cellura et al., 2015) (Eom et al., 2014) (Hidaka et al., 2012). No data are available in neurons and more specifically on TG1.

Selective TG1 inhibition can be technically challenging considering that TGs are well conserved and show high homology (Basso and Ratan, 2013). Blockage of TG1 activity could be an alternative strategy. Our results show that TG1 transcription in AD is driven by the AP1 responsive elements at the *TGM1* promoter. Both AP1 and AP2 levels and activity were found to be significantly upregulated in post-mortem AD brain samples as compared to non-AD brains (Vukic et al., 2009). The subunits of AP1 include members of Jun (c-jun, v-jun, jun-D and jun-B), fos (v-fos, c-fos, fos−B, fra-1, fra2) and activating transcription factor (ATF) (Karin et al., 1997) which are the key effectors of the c-jun N-terminal kinase (JNK)-signaling cascade. JNK is activated in response to a wide range of stimuli and its increased phosphorylation and activation have also been reported in post-mortem brains of AD patients (Zhu et al., 2001; Anderson et al., 1994; Thakur et al., 2007; Borsello and Forloni, 2007; Morishima et al., 2001). Consistently with our results, in keratinocytes differentiation, JNK activates the dual-leucine zipper bearing kinase (DLK) to induce the expression of TG1 (Robitaille et al., 2005). Pharmacological or peptide-based inhibition of JNK has been demonstrated to attenuate microglial activation and diminish the production of APP and Aβ fragment in AD models (Mehan et al., 2011; Colombo et al., 2007). Our results support the possibility that JNK inhibition protects neurons from Aβ toxicity also by halting neuronal TG1 upregulation.

4.2. Implications of TG1 silencing

Inhibitors of TGs have been shown to be protective in various neurodegenerative diseases (Keillor et al., 2015). We recently reported that dual inhibitors of HDAC and TG2 synergistically protect primary cortical neurons against oxidative stress (Basso et al., 2018). However, the use of TG1 inhibitors as a therapeutic option for AD needs to be considered carefully because TG1 is predominantly expressed in the skin (Basso and Ratan, 2013), and systemic reduction of TG1 activity might be toxic. Mutations in the *TGM1* gene lead to a loss of TG1 activity (Huber et al., 1995), associated with autosomal recessive congenital ichthyosis, a dermatological disease (Huber et al., 1995; Russell et al., 1995). Therefore, therapies should be designed to target and inhibit the stress-induced TG1 expression, while maintaining the basal expression of the protein. Further studies are warranted to decipher the role of TG1 and the other TG isoenzymes in the brain and their interplay in physiological and pathological conditions.

Concluding, we present TG1 as a new player of AD that is transcriptionally induced by Aβ 1–42 and is downstream of JNK activation. TG1 silencing protects neurons from Aβ toxicity and opens new opportunities for therapeutic intervention.

Acknowledgements

We would like to thank Dr. Massimo Pizzato's lab for help with the production and titration of lentiviruses; Michael Pancher at the High Throughput Screening Facility for assistance with the Operetta experiments; Sergio Robbiati at the Model Organism Facility; the Advanced Imaging Facility at Dep. CIBIO. This study was supported by the University of Trento and CIBIO (start-up funding to M.B.), the

Alzheimer Trento Onlus with the Legato Baldrachi (to M.B.).

Credit author statement

M.B. conceptualized the work; D.T., A.M., F.C., A.R., performed experiments in neurons, the real-time PCR in mouse tissues, all the western blotting, the cloning, viral transduction and transcriptional assays; P.G. performed the analysis with Operetta; F.F., L.B. D.A collected the tissues from the 3xTg mice; D.A. helped with the conceptualization of some experiments; L.G.H. and C.M. performed the electrophysiological experiments; L.C., M.S. provided the A < beta > peptides and the protocols to use the peptides; M.M.M.W. and B.D. perfomed the immunohistochemistry on 3xTg brains; D.T., M.P. and M.B. wrote the original draft; A.M. and M.B. reviewed and edited the resubmitted version of the manuscript. A.M. drew the graphical abstract. All co-authors read and approved the final version of the paper. M.B. provided funding for the majority of the experiments.

Appendix A. Supplementary data

Supplementary data to this article can be found online at https://doi.org/10.1016/j.nbd.2020.104849.

References

Akhter, R., Sanphui, P., Das, H., Saha, P., Biswas, S.C., 2015. The regulation of p53 up-regulated modulator of apoptosis by JNK/c-Jun pathway in beta-amyloid-induced neuron death. J. Neurochem. 134 (6), 1091–1103.

Anderson, A.J., Cummings, B.J., Cotman, C.W., 1994. Increased immunoreactivity for Jun- and Fos-related proteins in Alzheimer's disease: association with pathology. Exp. Neurol. 125 (2), 286–295.

Andre, W., Nondier, I., Valensi, M., Guillonneau, F., Federici, C., Hoffner, G., et al., 2017. Identification of brain substrates of transglutaminase by functional proteomics supports its role in neurodegenerative diseases. Neurobiol. Dis. 101, 40–58.

Appelt, D.M., Balin, B.J., 1997. The association of tissue transglutaminase with human recombinant tau results in the formation of insoluble filamentous structures. Brain Res. 745 (1–2), 21–31.

Bailey, C.D., Johnson, G.V., 2006. The protective effects of cystamine in the R6/2 Huntington's disease mouse involve mechanisms other than the inhibition of tissue transglutaminase. Neurobiol. Aging 27 (6), 871–879.

Bailey, C.D., Tucholski, J., Johnson, G.V., 2005. Transglutaminases in neurodegenerative disorders. Prog. Exp. Tumor Res. 38, 139–157.

Basso, M., Ratan, R.R., 2013. Transglutaminase is a therapeutic target for oxidative stress, excitotoxicity and stroke: a new epigenetic kid on the CNS block. J. Cereb. Blood Flow Metab. 33 (6), 809–818.

Basso, M., Berlin, J., Xia, L., Sleiman, S.F., Ko, B., Haskew-Layton, R., et al., 2012. Transglutaminase inhibition protects against oxidative stress-induced neuronal death downstream of pathological ERK activation. J. Neurosci. 32 (19), 6561–6569.

Basso, M., Chen, H.H., Tripathy, D., Conte, M., Apperley, K.Y.P., De Simone, A., et al., 2018. Designing dual transglutaminase 2/histone Deacetylase inhibitors effective at halting neuronal death. ChemMedChem 13 (3), 227–230.

Baumgartner, W., Golenhofen, N., Weth, A., Hiiragi, T., Saint, R., Griffin, M., et al., 2004. Role of transglutaminase 1 in stabilisation of intercellular junctions of the vascular endothelium. Histochem. Cell Biol. 122 (1), 17–25.

Borsello, T., Forloni, G., 2007. JNK signalling: a possible target to prevent neurodegeneration. Curr. Pharm. Des. 13 (18), 1875–1886.

Burguera, E.F., Love, B.J., 2006. Reduced transglutaminase-catalyzed protein aggregation is observed in the presence of creatine using sedimentation velocity. Anal. Biochem. 350 (1), 113–119.

Calderon-Garciduenas, A.L., Duyckaerts, C., 2017. Alzheimer disease. Handb. Clin. Neurol. 145, 325–337.

Caponi, S., Mattana, S., Ricci, M., Sagini, K., Urbanelli, L., Sassi, P., et al., 2016. Raman micro-spectroscopy study of living SH-SY5Y cells adhering on different substrates. Biophys. Chem. 208, 48–53.

Cellura, D., Pickard, K., Quaratino, S., Parker, H., Strefford, J.C., Thomas, G.J., et al., 2015. miR-19-mediated inhibition of Transglutaminase-2 leads to enhanced invasion and metastasis in colorectal Cancer. Mol. Cancer Res. 13 (7), 1095–1105.

Colombo, A., Repici, M., Pesaresi, M., Santambrogio, S., Forloni, G., Borsello, T., 2007. The TAT-JNK inhibitor peptide interferes with beta amyloid protein stability. Cell Death Differ. 14 (10), 1845–1848.

Eom, S., Kim, Y., Kim, M., Park, D., Lee, H., Lee, Y.S., et al., 2014. Transglutaminase II/microRNA-218/−181a loop regulates positive feedback relationship between allergic inflammation and tumor metastasis. J. Biol. Chem. 289 (43), 29483–29505.

Franich, N.R., Basso, M., Andre, E.A., Ochaba, J., Kumar, A., Thein, S., et al., 2018. Striatal mutant Huntingtin protein levels decline with age in homozygous Huntington's disease Knock-in mouse models. J. Huntingtons Dis. 7 (2), 137–150.

Grosso, H., Woo, J.M., Lee, K.W., Im, J.Y., Masliah, E., Junn, E., et al., 2014. Transglutaminase 2 exacerbates alpha-synuclein toxicity in mice and yeast. FASEB J. 28 (10), 4280–4291.

Halverson, R.A., Lewis, J., Frausto, S., Hutton, M., Muma, N.A., 2005. Tau protein is cross-linked by transglutaminase in P301L tau transgenic mice. J. Neurosci. 25 (5), 1226–1233.

Hidaka, H., Seki, N., Yoshino, H., Yamasaki, T., Yamada, Y., Nohata, N., et al., 2012. Tumor suppressive microRNA-1285 regulates novel molecular targets: aberrant expression and functional significance in renal cell carcinoma. Oncotarget 3 (1), 44–57.

Huber, M., Rettler, I., Bernasconi, K., Wyss, M., Hohl, D., 1995. Lamellar ichthyosis is genetically heterogeneous–cases with normal keratinocyte transglutaminase. J. Invest. Dermatol. 105 (5), 653–654.

de Jager, M., Drukarch, B., Hofstee, M., Breve, J., Jongenelen, C.A., Bol, J.G., et al., 2015. Tissue transglutaminase-catalysed cross-linking induces Apolipoprotein E multimers inhibiting Apolipoprotein E's protective effects towards amyloid-beta-induced toxicity. J. Neurochem. 134 (6), 1116–1128.

Jeitner, T.M., Muma, N.A., Battaile, K.P., Cooper, A.J., 2009a. Transglutaminase activation in neurodegenerative diseases. Future Neurol. 4 (4), 449–467.

Jeitner, T.M., Pinto, J.T., Krasnikov, B.F., Horswill, M., Cooper, A.J., 2009b. Transglutaminases and neurodegeneration. J. Neurochem. 109 (Suppl. 1), 160–166.

Jimenez Garduno, A.M., Juarez-Hernandez, L.J., Polanco, M.J., Tosatto, L., Michelatti, D., Arosio, D., et al., 2017. Altered ionic currents and amelioration by IGF-1 and PACAP in motoneuron-derived cells modelling SBMA. Biophys. Chem. 229, 68–76.

Junn, E., Ronchetti, R.D., Quezado, M.M., Kim, S.Y., Mouradian, M.M., 2003. Tissue transglutaminase-induced aggregation of alpha-synuclein: implications for Lewy body formation in Parkinson's disease and dementia with Lewy bodies. Proc. Natl. Acad. Sci. U. S. A. 100 (4), 2047–2052.

Kalinin, A., Marekov, L.N., Steinert, P.M., 2001. Assembly of the epidermal cornified cell envelope. J. Cell Sci. 114 (Pt 17), 3069–3070.

Karin, M., Liu, Z., Zandi, E., 1997. AP-1 function and regulation. Curr. Opin. Cell Biol. 9 (2), 240–246.

Keillor, J.W., Apperley, K.Y., Akbar, A., 2015. Inhibitors of tissue transglutaminase. Trends Pharmacol. Sci. 36 (1), 32–40.

Kim, S.Y., Grant, P., Lee, J.H., Pant, H.C., Steinert, P.M., 1999. Differential expression of multiple transglutaminases in human brain. Increased expression and cross-linking by transglutaminases 1 and 2 in Alzheimer's disease. J. Biol. Chem. 274 (43), 30715–30721.

Kumar, A., Kneynsberg, A., Tucholski, J., Perry, G., van Groen, T., Detloff, P.J., et al., 2012. Tissue transglutaminase overexpression does not modify the disease phenotype of the R6/2 mouse model of Huntington's disease. Exp. Neurol. 237 (1), 78–89.

Li, L., Watson, C.J., Dubourd, M., Bruton, A., Xu, M., Cooke, G., et al., 2016. HIF-1-dependent TGM1 expression is associated with maintenance of airway epithelial junction proteins. Lung 194 (5), 829–838.

Manzoni, C., Colombo, L., Messa, M., Cagnotto, A., Cantu, L., Del Favero, E., et al., 2009. Overcoming synthetic Abeta peptide aging: a new approach to an age-old problem. Amyloid 16 (2), 71–80.

Martinet, N., Bonnard, L., Regnault, V., Picard, E., Burke, L., Siat, J., et al., 2003. In vivo transglutaminase type 1 expression in normal lung, preinvasive bronchial lesions, and lung cancer. Am. J. Respir. Cell Mol. Biol. 28 (4), 428–435.

Mehan, S., Meena, H., Sharma, D., Sankhla, R., 2011. JNK: a stress-activated protein kinase therapeutic strategies and involvement in Alzheimer's and various neurodegenerative abnormalities. J. Mol. Neurosci. 43 (3), 376–390.

Menalled, L.B., Kudwa, A.E., Oakeshott, S., Farrar, A., Paterson, N., Filippov, I., et al., 2014. Genetic deletion of transglutaminase 2 does not rescue the phenotypic deficits observed in R6/2 and zQ175 mouse models of Huntington's disease. PLoS One 9 (6), e99520.

Morishima, Y., Gotoh, Y., Zieg, J., Barrett, T., Takano, H., Flavell, R., et al., 2001. Beta-amyloid induces neuronal apoptosis via a mechanism that involves the c-Jun N-terminal kinase pathway and the induction of Fas ligand. J. Neurosci. 21 (19), 7551–7560.

Munsie, L., Caron, N., Atwal, R.S., Marsden, I., Wild, E.J., Bamburg, J.R., et al., 2011. Mutant huntingtin causes defective actin remodeling during stress: defining a new role for transglutaminase 2 in neurodegenerative disease. Hum. Mol. Genet. 20 (10), 1937–1951.

Oddo, S., Caccamo, A., Shepherd, J.D., Murphy, M.P., Golde, T.E., Kayed, R., et al., 2003. Triple-transgenic model of Alzheimer's disease with plaques and tangles: intracellular Abeta and synaptic dysfunction. Neuron 39 (3), 409–421.

Olsson, T.T., Klementieva, O., Gouras, G.K., 2018. Prion-like seeding and nucleation of intracellular amyloid-beta. Neurobiol. Dis. 113, 1–10.

Phillips, M.A., Jessen, B.A., Lu, Y., Qin, Q., Stevens, M.E., Rice, R.H., 2004. A distal region of the human TGM1 promoter is required for expression in transgenic mice and cultured keratinocytes. BMC Dermatol. 4, 2.

Piccini, A., Borghi, R., Guglielmotto, M., Tamagno, E., Cirmena, G., Garuti, A., et al., 2012. Beta-amyloid 1-42 induces physiological transcriptional regulation of BACE1. J. Neurochem. 122 (5), 1023–1031.

Pizzato, M., McCauley, S.M., Neagu, M.R., Pertel, T., Firrito, C., Ziglio, S., et al., 2015. Lv4 is a capsid-specific antiviral activity in human blood cells that restricts viruses of the SIVMAC/SIVSM/HIV-2 lineage prior to integration. PLoS Pathog. 11 (7), e1005050.

Ponnusamy, M., Pang, M., Annamaraju, P.K., Zhang, Z., Gong, R., Chin, Y.E., et al., 2009. Transglutaminase-1 protects renal epithelial cells from hydrogen peroxide-induced apoptosis through activation of STAT3 and AKT signaling pathways. Am. J. Physiol. Renal. Physiol. 297 (5), F1361–F1370.

Robitaille, H., Proulx, R., Robitaille, K., Blouin, R., Germain, L., 2005. The mitogen-activated protein kinase kinase kinase dual leucine zipper-bearing kinase (DLK) acts as a key regulator of keratinocyte terminal differentiation. J. Biol. Chem. 280 (13), 12732–12741.

Roncador, A., Jimenez-Garduno, A.M., Pasquardini, L., Giusti, G., Cornella, N., Lunelli, L., et al., 2017. Primary cortical neurons on PMCS TiO2 films towards bio-hybrid

memristive device: a morpho-functional study. Biophys. Chem. 229, 115–122.
Russell, L.J., DiGiovanna, J.J., Rogers, G.R., Steinert, P.M., Hashem, N., Compton, J.G., et al., 1995. Mutations in the gene for transglutaminase 1 in autosomal recessive lamellar ichthyosis. Nat. Genet. 9 (3), 279–283.
Schmid, A.W., Condemi, E., Tuchscherer, G., Chiappe, D., Mutter, M., Vogel, H., et al., 2011. Tissue transglutaminase-mediated glutamine deamidation of beta-amyloid peptide increases peptide solubility, whereas enzymatic cross-linking and peptide fragmentation may serve as molecular triggers for rapid peptide aggregation. J. Biol. Chem. 286 (14), 12172–12188.
Selkoe, D.J., Abraham, C., Ihara, Y., 1982. Brain transglutaminase: in vitro crosslinking of human neurofilament proteins into insoluble polymers. Proc. Natl. Acad. Sci. U. S. A. 79 (19), 6070–6074.
Thakur, A., Wang, X., Siedlak, S.L., Perry, G., Smith, M.A., Zhu, X., 2007. C-Jun phosphorylation in Alzheimer disease. J. Neurosci. Res. 85 (8), 1668–1673.
Thomas, H., Beck, K., Adamczyk, M., Aeschlimann, P., Langley, M., Oita, R.C., et al., 2013. Transglutaminase 6: a protein associated with central nervous system development and motor function. Amino Acids 44 (1), 161–177.
Tripathy, D., Vignoli, B., Ramesh, N., Polanco, M.J., Coutelier, M., Stephen, C.D., et al., 2017. Mutations in TGM6 induce the unfolded protein response in SCA35. Hum. Mol. Genet. 26 (19), 3749–3762.
Van Raamsdonk, J.M., Pearson, J., Bailey, C.D., Rogers, D.A., Johnson, G.V., Hayden, M.R., et al., 2005. Cystamine treatment is neuroprotective in the YAC128 mouse model of Huntington disease. J. Neurochem. 95 (1), 210–220.
Vukic, V., Callaghan, D., Walker, D., Lue, L.F., Liu, Q.Y., Couraud, P.O., et al., 2009. Expression of inflammatory genes induced by beta-amyloid peptides in human brain endothelial cells and in Alzheimer's brain is mediated by the JNK-AP1 signaling pathway. Neurobiol. Dis. 34 (1), 95–106.
Wang, Y.H., Zhang, Y.G., 2018. Amyloid and immune homeostasis. Immunobiology 223 (3), 288–293.
Wilhelmus, M.M., Grunberg, S.C., Bol, J.G., van Dam, A.M., Hoozemans, J.J., Rozemuller, A.J., et al., 2009. Transglutaminases and transglutaminase-catalyzed cross-links co-localize with the pathological lesions in Alzheimer's disease brain. Brain Pathol. 19 (4), 612–622.
Wilhelmus, M.M., de Jager, M., Rozemuller, A.J., Breve, J., Bol, J.G., Eckert, R.L., et al., 2012. Transglutaminase 1 and its regulator tazarotene-induced gene 3 localize to neuronal tau inclusions in tauopathies. J. Pathol. 226 (1), 132–142.
Zhang, W., Johnson, B.R., Suri, D.E., Martinez, J., Bjornsson, T.D., 1998. Immunohistochemical demonstration of tissue transglutaminase in amyloid plaques. Acta Neuropathol. 96 (4), 395–400.
Zhang, Z., Xing, J., Ma, L., Gong, R., Chin, Y.E., Zhuang, S., 2009. Transglutaminase-1 regulates renal epithelial cell proliferation through activation of Stat-3. J. Biol. Chem. 284 (5), 3345–3353.
Zhang, J., Wang, S., Huang, W., Bennett, D.A., Dickson, D.W., Wang, D., et al., 2016. Tissue transglutaminase and its product Isopeptide are increased in Alzheimer's disease and APPswe/PS1dE9 double transgenic mice brains. Mol. Neurobiol. 53 (8), 5066–5078.
Zhu, X., Castellani, R.J., Takeda, A., Nunomura, A., Atwood, C.S., Perry, G., et al., 2001. Differential activation of neuronal ERK, JNK/SAPK and p38 in Alzheimer disease: the 'two hit' hypothesis. Mech. Ageing Dev. 123 (1), 39–46.